



## OPEN ACCESS

## EDITED BY

Yongfeng Guo,  
Chinese Academy of Agricultural  
Sciences, China

## REVIEWED BY

Chen Meng,  
Chinese Academy of Agricultural  
Sciences, China  
Ahmed A. A. Aioub,  
Zagazig University, Egypt

## \*CORRESPONDENCE

Songbiao Chen

✉ sbchen@fjage.org

Wenqing Li

✉ li-wqfjyc@163.com

†These authors contributed  
equally to this work and share  
first authorship

RECEIVED 19 August 2024

ACCEPTED 06 November 2024

PUBLISHED 25 November 2024

## CITATION

Liang T, Lin J, Wu S, Ye R, Qu M, Xie R, Lin Y,  
Gao J, Wang Y, Ke Y, Li C, Guo J, Lu J,  
Tang W, Chen S and Li W (2024) Integrative  
transcriptomic analysis reveals the molecular  
responses of tobacco to magnesium  
deficiency.

*Front. Plant Sci.* 15:1483217.

doi: 10.3389/fpls.2024.1483217

## COPYRIGHT

© 2024 Liang, Lin, Wu, Ye, Qu, Xie, Lin, Gao,  
Wang, Ke, Li, Guo, Lu, Tang, Chen and Li. This  
is an open-access article distributed under the  
terms of the [Creative Commons Attribution  
License \(CC BY\)](#). The use, distribution or  
reproduction in other forums is permitted,  
provided the original author(s) and the  
copyright owner(s) are credited and that the  
original publication in this journal is cited, in  
accordance with accepted academic  
practice. No use, distribution or reproduction  
is permitted which does not comply with  
these terms.

# Integrative transcriptomic analysis reveals the molecular responses of tobacco to magnesium deficiency

Tingmin Liang<sup>1,2,3†</sup>, Jinbin Lin<sup>2†</sup>, Shengxin Wu<sup>1</sup>, Rongrong Ye<sup>2</sup>,  
Mengyu Qu<sup>2,4</sup>, Rongrong Xie<sup>1,5</sup>, Yingfeng Lin<sup>2</sup>, Jingjuan Gao<sup>1,5</sup>,  
Yuemin Wang<sup>1</sup>, Yuqin Ke<sup>6</sup>, Chunying Li<sup>1</sup>, Jinping Guo<sup>1</sup>,  
Jianjun Lu<sup>2</sup>, Weiqi Tang<sup>2</sup>, Songbiao Chen<sup>2\*</sup> and Wenqing Li<sup>1\*</sup>

<sup>1</sup>Institute of Tobacco Sciences, Fujian Provincial Tobacco Monopoly Bureau, Fuzhou, China, <sup>2</sup>Ministerial and Provincial Joint Innovation Centre for Safety Production of Cross-Strait Crops, College of Geography and Oceanography, Minjiang University, Fuzhou, China, <sup>3</sup>College of Agriculture, Fujian Agriculture and Forestry University, Fuzhou, China, <sup>4</sup>College of Plant Protection, Fujian Agriculture and Forestry University, Fuzhou, China, <sup>5</sup>International Magnesium Institute, Fujian Agriculture and Forestry University, Fuzhou, China, <sup>6</sup>College of Life Science, Fujian Agriculture and Forestry University, Fuzhou, China

**Introduction:** Magnesium (Mg) is a crucial macronutrient for plants. Understanding the molecular responses of plants to different levels of Mg supply is important for improving cultivation practices and breeding new varieties with efficient Mg utilization.

**Methods:** In this study, we conducted a comprehensive transcriptome analysis on tobacco (*Nicotiana tabacum* L.) seedling leaves to investigate changes in gene expression in response to different levels of Mg supply, including Mg-deficient, 1/4-normal Mg, normal Mg, and 4x-normal Mg, with a particular focus on Mg deficiency at 5, 15 and 25 days after treatment (DAT), respectively.

**Results:** A total of 11,267 differentially expressed genes (DEGs) were identified in the Mg-deficient, 1/4-normal Mg, and/or 4x-normal Mg seedlings compared to the normal Mg seedlings. The global gene expression profiles revealed potential mechanisms involved in the response to Mg deficiency in tobacco leaves, including down-regulation of genes—two DEGs encoding mitochondria-localized NtMGT7 and NtMGT9 homologs, and one DEG encoding a tonoplast-localized NtMHX1 homolog—associated with Mg trafficking from the cytosol to mitochondria and vacuoles, decreased expression of genes linked to photosynthesis and carbon fixation at later stages, and up-regulation of genes related to antioxidant defenses, such as *NtPODs*, *NtPrxs*, and *NtGSTs*.

**Discussion:** Our findings provide new insights into the molecular mechanisms underlying how tobacco responds to Mg deficiency.

## KEYWORDS

tobacco, magnesium, transcriptome analysis, Mg<sup>2+</sup> transporter, Mg<sup>2+/H+</sup> exchanger, photosynthesis, antioxidant response

## 1 Introduction

Magnesium (Mg) is an essential macronutrient for plants, vital for photosynthesis, enzyme activation, protein synthesis, and nucleotide metabolism (Cowan, 2002; Chaudhry et al., 2021). As the central atom in the chlorophyll molecule, Mg plays a crucial role in various processes such as chlorophyll biosynthesis, photosynthetic metabolism, and CO<sub>2</sub> assimilation (Verbruggen and Hermans, 2013). Additionally, Mg acts as a cofactor and allosteric modulator for a variety of enzymes, including carboxylases, phosphatases, protein kinases, RNA polymerases, and ATPases (Shaul, 2002), therefore influencing various physiological, biochemical, and cellular processes for plant growth and development (Cakmak and Kirkby, 2008).

Mg is one of the most abundant elements in the Earth's crust. However, the majority of soil Mg (90-98%) is incorporated into various minerals and is not directly available to plants (Senbayram et al., 2015). The form of Mg that plant can absorb is Mg<sup>2+</sup>. Due to its small ionic radius but large hydrated radius, Mg<sup>2+</sup> binds weakly to negatively charged soil colloids and is easily leached from acidic and sandy soils (Verbruggen and Hermans, 2013), resulting in Mg deficiency in agricultural lands worldwide (Maathuis, 2009). Mg deficiency reduces chlorophyll biosynthesis, causes photooxidative damage, and impairs the phloem loading of photoassimilates in plants (Chaudhry et al., 2021). Common morphological symptoms of Mg deficiency in plants include growth retardation and interveinal leaf chlorosis (Marschner and Cakmak, 1989; Cakmak and Kirkby, 2008). Ultimately, Mg deficiency leads to significant reductions in crop yield and quality (Moss and Higgins, 1974; Cakmak, 2013).

While Mg deficiency has been a prevalent issue in agriculture, it has gained significant attention in recent decades (Hauer-Jäkli and Tränkner, 2019). In recent years, an increasing number of studies have focused on investigating the physiological and molecular mechanisms underlying plant responses to Mg deficiency (Ishfaq et al., 2022; Tang et al., 2022; Deng et al., 2023; Wang et al., 2023). However, the detailed mechanism remains incompletely understood. Tobacco (*Nicotiana tabacum* L.) is an important model in plant biology and is a significant economic crop. Mg is vital for the growth and development of tobacco. Mg deficiency is prevalent in soils suited for tobacco cultivation, leading to decreased yield and quality (Liu et al., 1998; Li et al., 2022). Several studies have demonstrated that the proper application of Mg fertilizers enhances the growth, development, yield, and leaf quality of flue-cured tobacco (Liu et al., 1998; Xu et al., 2011; Li et al., 2022, 2023). However, there is limited knowledge regarding the molecular response mechanism of tobacco to Mg deficiency. In the present study, we performed an RNA-Seq analysis on tobacco seedlings grown under Mg deficiency and at three different levels of Mg supply. Our results revealed dynamic changes in gene expression in response to Mg deficiency in tobacco leaves, including down-regulation of genes involved in Mg trafficking from the cytosol to mitochondria and vacuoles, decreased expression of genes related to photosynthesis and carbon fixation at later stages, and up-regulation of genes associated with antioxidant defenses.

## 2 Materials and methods

### 2.1 Plant materials and growth conditions

Tobacco (*Nicotiana tabacum* L. cv. CB-1) seedlings were first germinated in soil trays and grown under standard conditions for approximately 5-6 weeks, until they reached the seven-leaf stage. Subsequently, tobacco seedlings were transferred from soil trays to 1000 mL plastic boxes filled with a modified Hoagland nutrient solution. The nutrient solution consisted of the following components: 4.66 mM Ca(NO<sub>3</sub>)<sub>2</sub>·4H<sub>2</sub>O, 1.41 mM KH<sub>2</sub>PO<sub>4</sub>, 4.98 mM KNO<sub>3</sub>, 1.99 mM MgSO<sub>4</sub>·7H<sub>2</sub>O, 0.10 mM FeSO<sub>4</sub>·7H<sub>2</sub>O, 0.10 mM EDTA-2Na, 46.26 μM H<sub>3</sub>BO<sub>3</sub>, 9.10 μM MnCl<sub>2</sub>·4H<sub>2</sub>O, 0.77 μM ZnCl<sub>2</sub>, 0.41 μM CuCl<sub>2</sub>·2H<sub>2</sub>O, and 0.13 μM Na<sub>2</sub>MoO<sub>4</sub>·2H<sub>2</sub>O (Lu et al., 2023).

After a pre-culture of one week in growth chambers under a 12-hour light at 25°C/12-hour dark at 20°C, the well-grown tobacco seedlings were transferred to new plastic boxes and cultured in the modified Hoagland nutrient solutions with the Mg concentrations of Mg-deficient (0 mM), 1/4-normal Mg (0.50 mM), normal Mg (1.99 mM), and 4×-normal Mg (7.96 mM) (hereafter designated as Mg0, Mg1/4, Mg1, and Mg4), respectively. Tobacco seedlings were maintained in the growth chambers under the same light-dark cycle and temperature conditions as during the pre-culture phase. The liquid solutions in the plastic boxes were completely replaced every three days to ensure fresh nutrients for the seedlings. Each treatment group consisted of three replicates, with each replicate containing three seedlings.

### 2.2 Measurement of physiological traits

The first fully expanded leaf of tobacco seedlings grown under different levels of Mg supply was sampled at 25 days after treatment (DAT). A total of 14 physiological parameters were measured, including the contents of Mg, chlorophyll a (Chla), chlorophyll b (Chlb), carotenoids (Car), soluble proteins (SP), and hydrogen peroxide (H<sub>2</sub>O<sub>2</sub>); the activities of ribulose-1,5-bisphosphate carboxylase (RuBPCase), acid invertase (AI), neutral invertase (NI), nitrate reductase (NR), superoxide dismutase (SOD), catalase (CAT), and peroxidase (POD); root vitality; as well as cell membrane permeability (CMP). Each experiment had three biological replicates.

The measurements were conducted following established methods as previously described (Lu et al., 2023). Specifically, the content of Mg was determined using inductively coupled plasma optical emission spectroscopy (ICP-OES) system (iCAP 7000 Series, Thermo Fisher Scientific, USA) (Musharraf et al., 2012). The contents of Chla, Chlb, and Car were measured using a spectrophotometer, as per the protocol by Lichtenthaler and Buschmann (2001); SP and H<sub>2</sub>O<sub>2</sub> levels were quantified following the procedures described by Anderson et al. (1995) and by Clemensson-Lindell (1994), respectively; RuBPCase activity was measured following the procedure described by Leech et al.

(1985), while AI, NI, NR, SOD, CAT, and POD activities were assessed using Zou's methodologies (Zou, 2000); root vitality was determined using the triphenyltetrazolium chloride (TTC) method (Clemensson-Lindell, 1994); lastly, CMP of leaves was determined through electrolyte leakage, as described by Palta and Stadelmann (1997).

### 2.3 RNA-seq analysis

The first fully expanded leaf of tobacco seedlings grown in nutrient solutions with different levels of Mg supply was collected at 5, 15, and 25 DAT, respectively, for RNA-Seq analysis. Each treatment consisted of three independent biological replicates, with one seedling per replicate. Total RNA was extracted from finely ground leaf samples using TRIzol reagent (Thermo Fisher Scientific, China). The extracted RNA was treated with RNase-free DNase I (Thermo Fisher Scientific, China) to eliminate genomic DNA contamination. The RNA samples were then subjected to RNA-Seq analysis at Novogene, Beijing, China, using an Illumina Novaseq platform.

The resulting sequencing data was processed and were mapped to the reference genome of tobacco available at [https://solgenomics.net/organism/Nicotiana\\_tabacum/genome](https://solgenomics.net/organism/Nicotiana_tabacum/genome), using the HISAT2 v2.0.5 program (Kim et al., 2015). The expression level of each gene was quantified based on the fragments per kilobase of transcript per million mapped reads (FPKM) value (Trapnell et al., 2010). Differential expression analysis was performed using the DESeq2 package in R platform (Love et al., 2014). Genes with a  $|\log_2 FC| \geq 1$  and the false discovery rate (FDR)  $\leq 0.05$  were considered as differentially expressed genes (DEGs).

### 2.4 Gene ontology and Kyoto encyclopedia of genes and genomes analysis

The identified DEGs were subjected to GO analysis using the Goseq R packages (Young et al., 2010), and to KEGG pathway enrichment analysis using the KEGG Orthology-based Annotation System (KOBAS) software (Xie et al., 2011). GO terms or KEGG pathways with  $p \leq 0.05$  were considered for further assessment in this study.

### 2.5 Real-time quantitative RT-PCR

Total RNAs were extracted from tobacco leaves using the TransZol Up kit (TransGen Biotech, China) and were treated with RNase-free DNase I (Takara, China) to eliminate any contaminating DNA. First-strand cDNA synthesis was then performed using a HiScript II 1st Strand cDNA Synthesis Kit (Vazyme, China). Quantitative real-time PCR (qRT-PCR) reactions were carried out on a CFX Connect Real-Time System (BIO-RAD, USA) with a SYBR qPCR Master Mix (Vazyme, China). Three replications were conducted for each sample. Internal control tests were conducted with the tobacco *EF-1 $\alpha$*  gene (Schmidt and Delaney, 2010). Relative expression values

were calculated using the  $2^{-\Delta\Delta CT}$  method (Livak and Schmittgen, 2001). The transcriptional profiles of 11 DEGs involved in Mg distribution and antioxidative regulation were validated using qRT-PCR. The specific primers used for the qRT-PCR analysis can be referenced in Supplementary Table S1.

## 2.6 Subcellular localization

The open reading fragment (ORF) sequences of the target genes were obtained from the Solanaceae Genomics Network ([https://solgenomics.net/ftp/genomes/Nicotiana\\_tabacum/edwards\\_et\\_al\\_2017/](https://solgenomics.net/ftp/genomes/Nicotiana_tabacum/edwards_et_al_2017/)). Subcellular localization constructs for the homologous NtMGT7 (Nitab4.5\_0003331g0150) and NtMGT9 (Nitab4.5\_0000436g0030), and the homologous NtMHX1 (Nitab4.5\_0005805g0040), were created by amplifying and inserting the ORFs of these genes into pCS-NGFP (Qu et al., 2021) to fuse with the *GFP* gene. The resulting constructs were then introduced into the *Agrobacterium tumefaciens* strain GV3101. The GV3101 bacteria carrying these GFP-fusion constructs, a mitochondria ScCOX4-DsRed marker construct or a tonoplast *Oxy-TIP*-DsRed marker construct (Chen et al., 2019) were cultured in liquid yeast extract peptone media supplemented with kanamycin (50  $\mu$ g/ml) and rifampicin (50  $\mu$ g/ml). Suspensions of the GV3101 bacteria containing the GFP-fusion constructs were co-infiltrated with the DsRed marker constructs into leaves of 4-week-old *Nicotiana benthamiana* plants grown in a growth chamber at 25°C under a 16/8 h light/dark cycle. The infiltrated plants were maintained in darkness at 25°C for 3 days. The infiltrated leaf tissues were collected and used to isolate protoplasts. Fluorescence microscopy was conducted on the *N. benthamiana* protoplasts using a Leica DMI8 Laser Scanning Confocal microscope (STELLARIS 5, Leica, Germany) with Excitation/emission wavelengths 488/535 nm for green fluorescence, and 552/610 nm for red fluorescence.

## 3 Results

### 3.1 Mg deficiency inhibits growth of tobacco seedlings

Tobacco seedlings were grown in modified Hoagland's nutrient solutions supplied with four different levels of Mg (Mg0, Mg1/4, Mg1, and Mg4, respectively). At 5 DAT, no significant morphological differences were observed among the seedlings (data not shown). However, by 15 DAT, the Mg0 seedlings showed slight growth stunting, and by 25 DAT, they exhibited symptoms of leaf chlorosis and curling (Figure 1A). In contrast, the Mg1/4, Mg1, and Mg4 seedlings did not show noticeable morphological differences at either 15 or 25 DAT (Figure 1A).

At 25 DAT, the Mg content and eight physiological traits related to photosynthesis, carbon, and nitrogen metabolism in leaves of tobacco seedlings grown under different Mg levels were assessed. The Mg content in the Mg0 seedlings were notably lower compared to that in the Mg1/4, Mg1, and Mg4 seedlings (Figure 1B). The

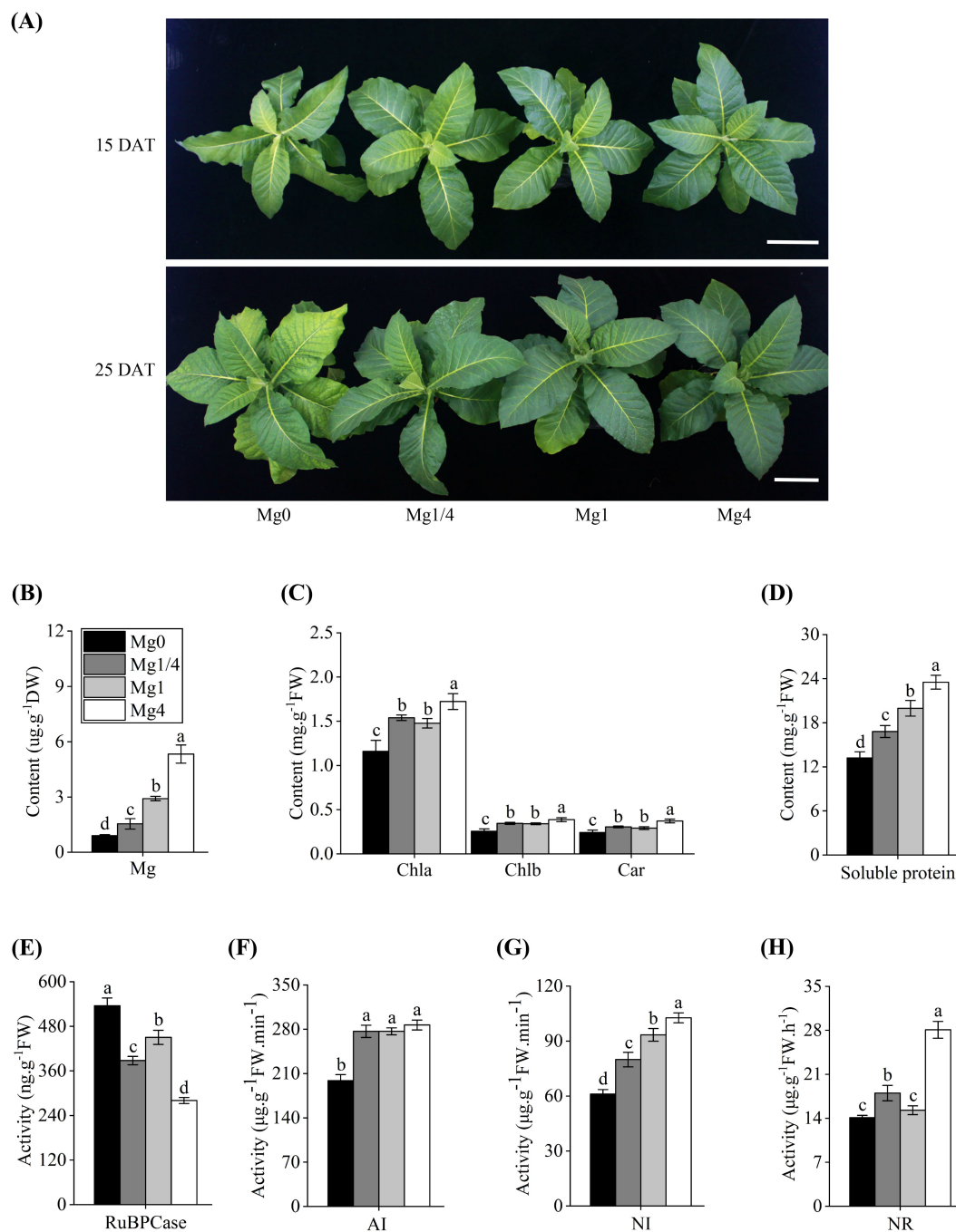


FIGURE 1

Effects of different Mg supply levels on growth and physiological parameters of tobacco seedlings. **(A)** Phenotype of tobacco seedlings grown under different Mg supply levels at 15 and 25 DAT (days after treatment), respectively. Scale bars = 10 cm. Mg0, 0 mM Mg; Mg1/4, 0.50 mM Mg; Mg1, 1.99 mM Mg; Mg4, 7.96 mM Mg. **(B)** Magnesium (Mg) content in leaves of tobacco seedlings grown under different Mg supplies at 25 DAT. **(C)** Contents of chlorophyll a (Chla), chlorophyll b (Chlb), and carotenoids (Car) in leaves of tobacco seedlings grown under different Mg supplies at 25 DAT. **(D)** Concentration of soluble proteins (SP) in leaves of tobacco seedlings grown under different Mg supplies at 25 DAT. **(E)** Content of RuBPCase in leaves of tobacco seedlings grown under different Mg supplies at 25 DAT. **(F-H)** Activities of acid invertase (AI), neutral invertase (NI), and nitrate reductase (NR) in leaves of tobacco seedlings grown under different Mg supplies at 25 DAT. Different letters (a, b, c, d) above the columns indicate statistical differences ( $p < 0.05$ ).

contents of three essential photosynthetic pigments (Chla, Chlb, and Car) in the Mg0 seedlings were significantly lower compared to those in the Mg1/4, Mg1, and Mg4 seedlings (Figure 1C). Similarly, the content of SP, an important osmoregulatory substance, was notably reduced in the Mg0 seedlings than in the Mg1/4, Mg1, and

Mg4 seedlings (Figure 1D). In contrast, the activity of RuBPCase, a key C3 enzyme responsible for carbon fixation, was markedly higher in the Mg0 seedlings compared to the Mg1/4, Mg1, and Mg4 seedlings (Figure 1E). Furthermore, the activities of AI and NI, both involved in carbon metabolism, were significantly reduced in

the Mg0 seedlings compared to the Mg1/4, Mg1, and Mg4 seedlings (Figures 1F, G). Similarly, the activity of NR, a crucial enzyme in nitrogen metabolism, was lower in the Mg0 seedlings than in the Mg1/4 and Mg4 seedlings (Figure 1H). These results demonstrated that a deficiency of Mg causes severe physiological disorders and inhibits the growth of tobacco seedlings.

### 3.2 Transcriptome profiling of genes showing differential expression in response to different levels of Mg supply

To investigate the molecular responses of tobacco plants to different levels of Mg supply, leaves from the Mg0, Mg1/4, Mg1, and Mg4 seedlings were collected at 5, 15, and 25 DAT, respectively, for RNA-Seq analysis. A total of 11,267 DEGs were identified in the Mg0, Mg1/4, and/or Mg4 seedlings compared to the Mg1 seedlings (Supplementary Table S2). While only a small number of DEGs were identified at 5 DAT (41 in Mg0, 38 in Mg1/4, and 13 in Mg4), a significantly higher number of DEGs were identified at 15 DAT (4,357 in Mg0, 910 in Mg1/4, and 482 in Mg4), and 25 DAT (6,376 in Mg0, 303 in Mg1/4, and 2,440 in Mg4), respectively (Figure 2A; Supplementary Table S3). Heatmap analysis revealed similar transcriptomic profiles for the Mg0, Mg1/4, Mg1, and Mg4 seedlings at 5 DAT, but more distinct differences emerged at 15 and 25 DAT, especially between the Mg0 seedlings and the other groups (Figure 2B).

Additionally, an upset analysis was conducted on the DEGs identified in the Mg0, Mg1/4, and/or Mg4 seedlings compared to the Mg1 seedlings to gain deeper insights into the regulation patterns of these DEGs in tobacco seedlings grown under various Mg levels over different growth durations (Figure 2C). For example, approximately 2,132 and 4,405 DEGs were specifically regulated in the Mg0 seedlings at 15 and 25 DAT, respectively, while 1,022 DEGs were co-regulated in the Mg0 seedlings at both 15 DAT and 25 DAT. In contrast, only 11 DEGs were specifically regulated in the Mg0 seedlings at 5 DAT, with eight DEGs co-regulated at both 5 DAT and 15 DAT, and five DEGs co-regulated at both 5 DAT and 25 DAT (Figure 2C). The results highlight that a significant number of genes were markedly induced in tobacco seedlings in response to Mg deficiency after 15 days of growth, with certain DEGs showing relatively long-term regulation.

### 3.3 DEGs involved in Mg distribution

Plants have developed mechanisms to transport and distribute Mg to maintain optimal cellular levels (Tang and Luan, 2017). Mg<sup>2+</sup> transporters (MGTs) play essential roles in Mg uptake, transport and distribution (Yan et al., 2018). Among the DEGs identified, one *MGT7* homologous gene (*Nitab4.5\_0003331g0150*) and one *MGT9* homologous gene (*Nitab4.5\_0000436g0030*) were found to be down-regulated in the Mg0 seedlings at 25 DAT (Figure 3A). Mg<sup>2+</sup>/H<sup>+</sup> exchanger (MHX) has been shown to facilitate Mg<sup>2+</sup> influx into the vacuole (Shaul et al., 1999). A homologous *MHX1* gene (*Nitab4.5\_0005805g0040*) was also identified as a DEG that was

down-regulated in the Mg0 seedlings at 25 DAT (Figure 3B). To validate the transcriptome results, qRT-PCR analysis was conducted on the homologous *NtMGT7*, *NtMGT9*, and *NtMHX1* gene in the Mg0, Mg1/4, Mg1, and Mg4 seedlings at 25 DAT. The results indicated a significant down-regulation of all three genes in the Mg0 seedlings, consistent with the RNA-Seq data (Figures 3C-E).

The subcellular localization of MGTs and MHX is closely associated with their roles in the biological processes occurring within respective organelles. To investigate the subcellular localization of the homologous *NtMGT7*, *NtMGT9* and *NtMHX1* proteins, transient expression of the *NtMGT7-GFP*, *NtMGT9-GFP*, and *NtMHX1-GFP* fusions was conducted in *N. benthamiana* cells. The results demonstrated that the green fluorescence of *NtMGT7-GFP*, and *NtMGT9-GFP* co-localized with the mitochondria *ScCOX4-DsRed* marker (Figure 3F), indicating that both *NtMGT7* and *NtMGT9* are localized in the mitochondria. On the other hand, the green fluorescence of *NtMHX1-GFP* merged with the tonoplast *Osy-TIP-DsRed* marker (Figure 3F), suggesting that *NtMHX1* is localized to the vacuole membrane. These observations provide insights into the specific subcellular locations of *NtMGT7*, *NtMGT9* and *NtMHX1* and their respective roles within the cell.

### 3.4 DEGs involved in photosynthesis

To further understand the molecular mechanisms underlying tobacco's response to different levels of Mg supply, a KEGG analysis was conducted on the DEGs from the Mg0, Mg1/4, and Mg4 seedlings compared to the Mg1 seedlings. The analysis revealed that both the up- and down-regulated DEGs in the Mg0, Mg1/4, and Mg4 seedlings were enriched in diverse pathways, particularly at 15 and 25 DAT. Significantly, multiple KEGG pathways associated with photosynthesis were prominently highlighted, including photosynthesis, photosynthesis-antenna proteins, and carbon fixation in photosynthetic organisms (Supplementary Table S4).

The KEGG photosynthesis pathway was significantly enriched among the up-regulated DEGs in the Mg0 seedlings at 15 DAT, as well as among the down-regulated DEGs in the Mg0 seedlings and the up-regulated DEGs in the Mg4 seedlings at 25 DAT (Supplementary Table S4). The DEGs encoding proteins related to processes involved in the KEGG photosynthesis pathway, including photosystem II (PSII), photosystem I (PSI), photosynthetic electron transport, and F-type ATPase, were summarized (Figure 4A). A total of 45 DEGs related to the photosynthesis pathway were identified, with 32 up-regulated in the Mg0 seedlings at 15 DAT, nine down-regulated in the Mg0 seedlings at 25 DAT, and nine up-regulated in the Mg4 seedlings at 25 DAT (Figure 4B).

The KEGG pathway of photosynthesis-antenna proteins was significantly enriched among the up-regulated DEGs in the Mg4 seedlings at 25 DAT (Supplementary Table S4). There were four DEGs related to the light-harvesting chlorophyll protein complex, all of which were up-regulated in the Mg4 seedlings at 25 DAT (Figures 5A, B). Additionally, the KEGG pathway of carbon fixation in photosynthetic organisms was significantly enriched among the up-regulated DEGs in the Mg0 seedlings at 15 DAT, and the down-regulated DEGs in the Mg0 seedlings at 25 DAT (Supplementary

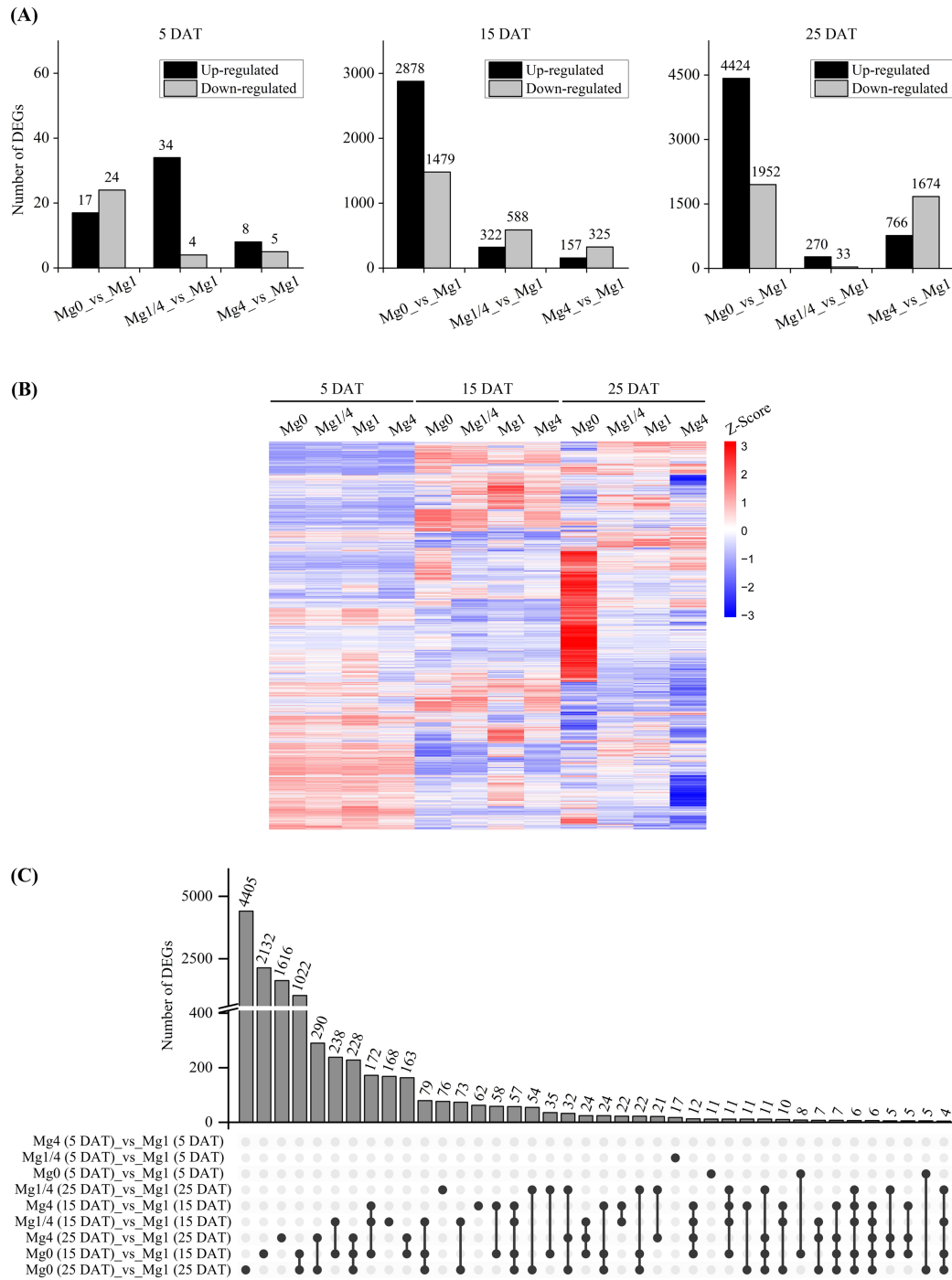


**FIGURE 2** Overview of the differentially expressed genes (DEGs) in leaves of tobacco seedlings in response to different Mg supplies. **(A)** Number of the up-regulated and down-regulated DEGs in Mg0, Mg1/4, and Mg4 in comparison to Mg1 at 5, 15, and 25 DAT, respectively. **(B)** Heatmap showing the differential expression levels of the identified DEGs in leaves of tobacco seedlings grown under different Mg supplies at 5, 15, and 25 DAT, respectively. **(C)** Upset diagram showing the numbers of the DEGs specific or common in leaves of tobacco seedlings grown under different Mg supplies at 5, 15, and 25 DAT, respectively. Mg0, 0 mM Mg; Mg1/4, 0.50 mM Mg; Mg1, 1.99 mM Mg; Mg4, 7.96 mM Mg.

**Table S4**). A total of 26 DEGs related to processes (C4-Dicarboxylic acid cycle and reductive pentose phosphate cycle) involved in the carbon fixation in the photosynthetic organisms pathway were identified within this pathway. Of these, 15 DEGs were up-regulated in the Mg0 seedlings at 15 DAT, while 12 were down-regulated in the Mg0 seedlings at 25 DAT (Figures 6A, B).

### 3.5 DEGs involved in antioxidative regulation

Plant leaves that are deficient in Mg are highly photosensitive, leading to an over-saturation of photosynthetic electron transport system. Under highly reduced condition, electrons could pass-on

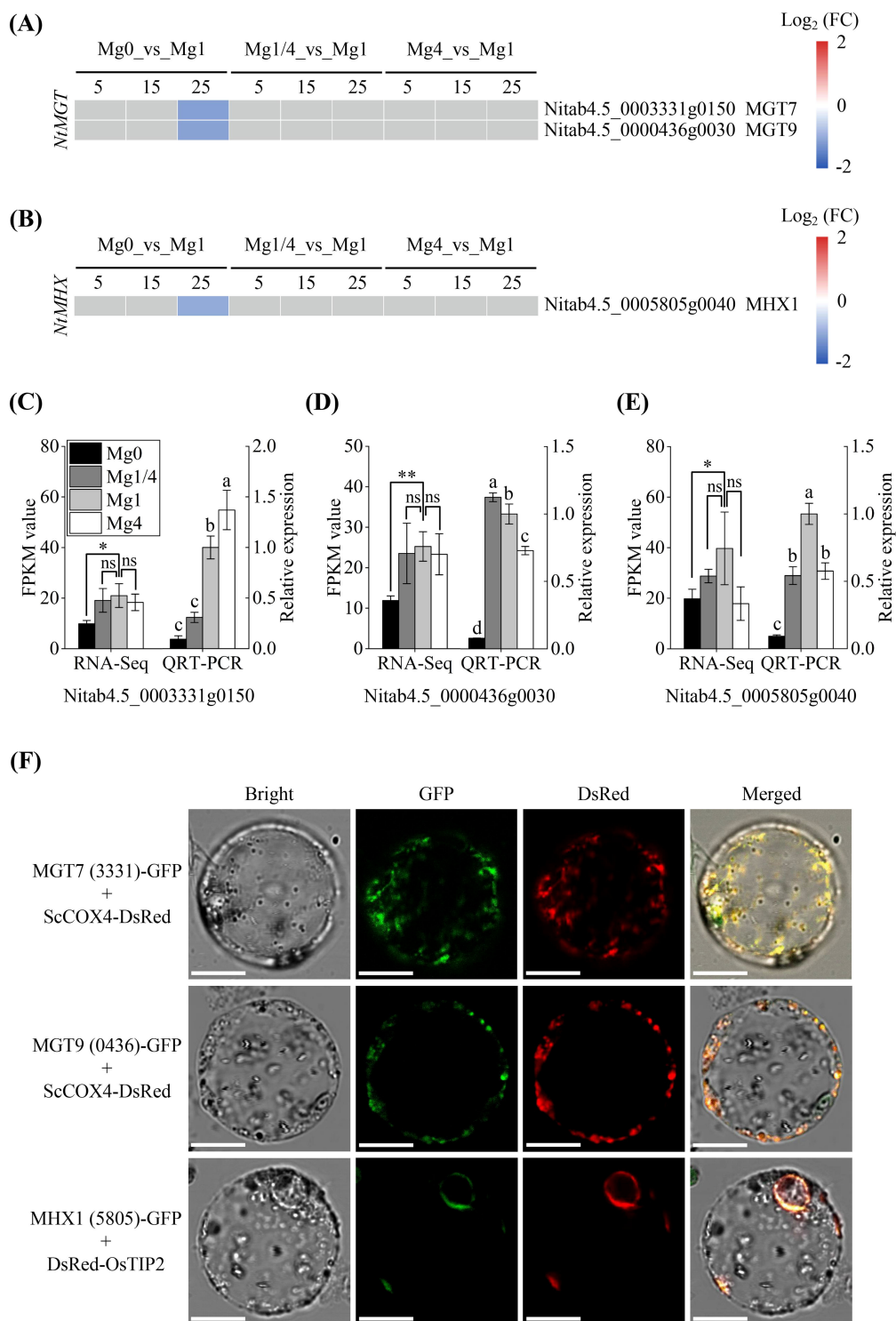
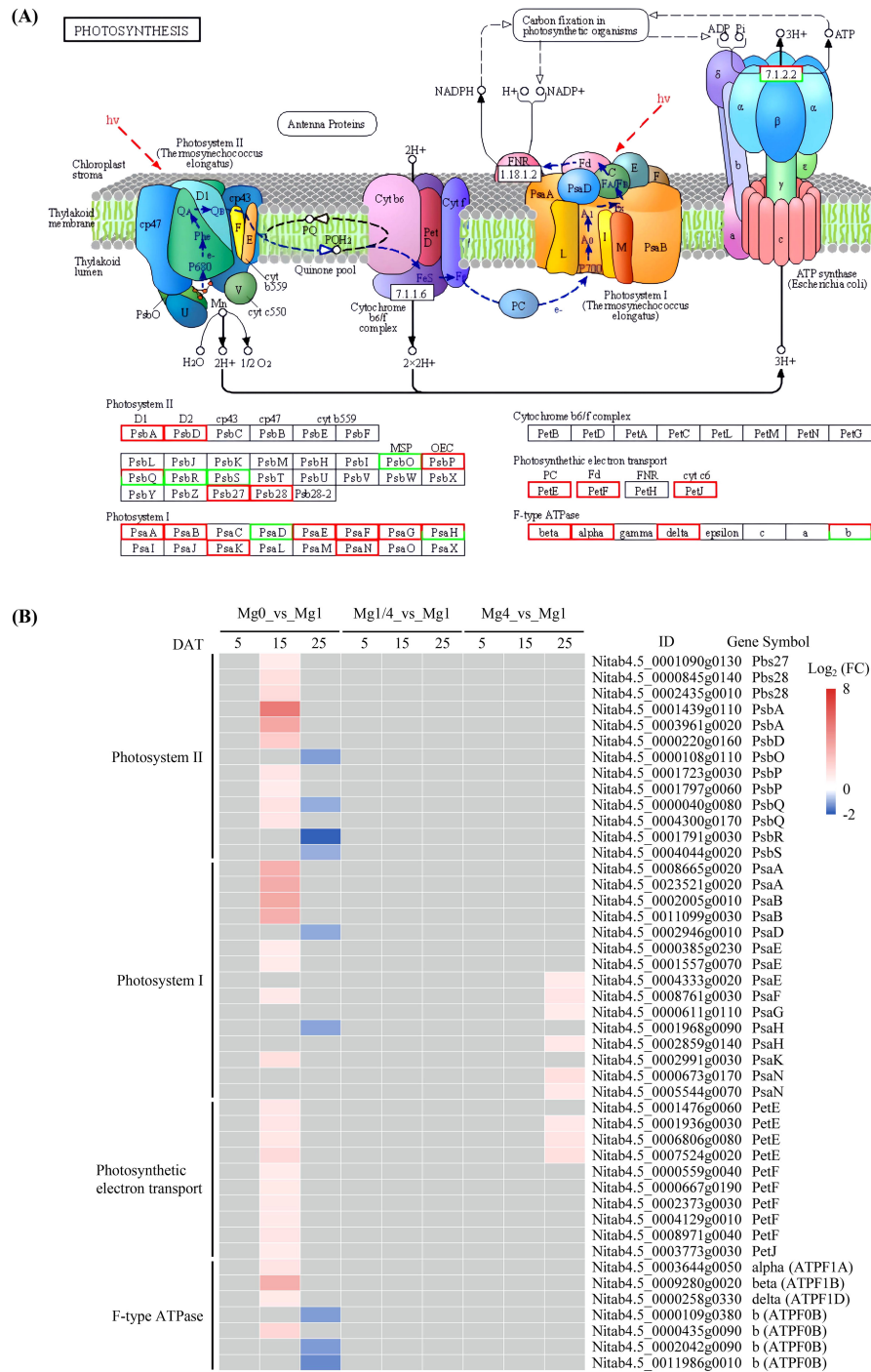


FIGURE 3

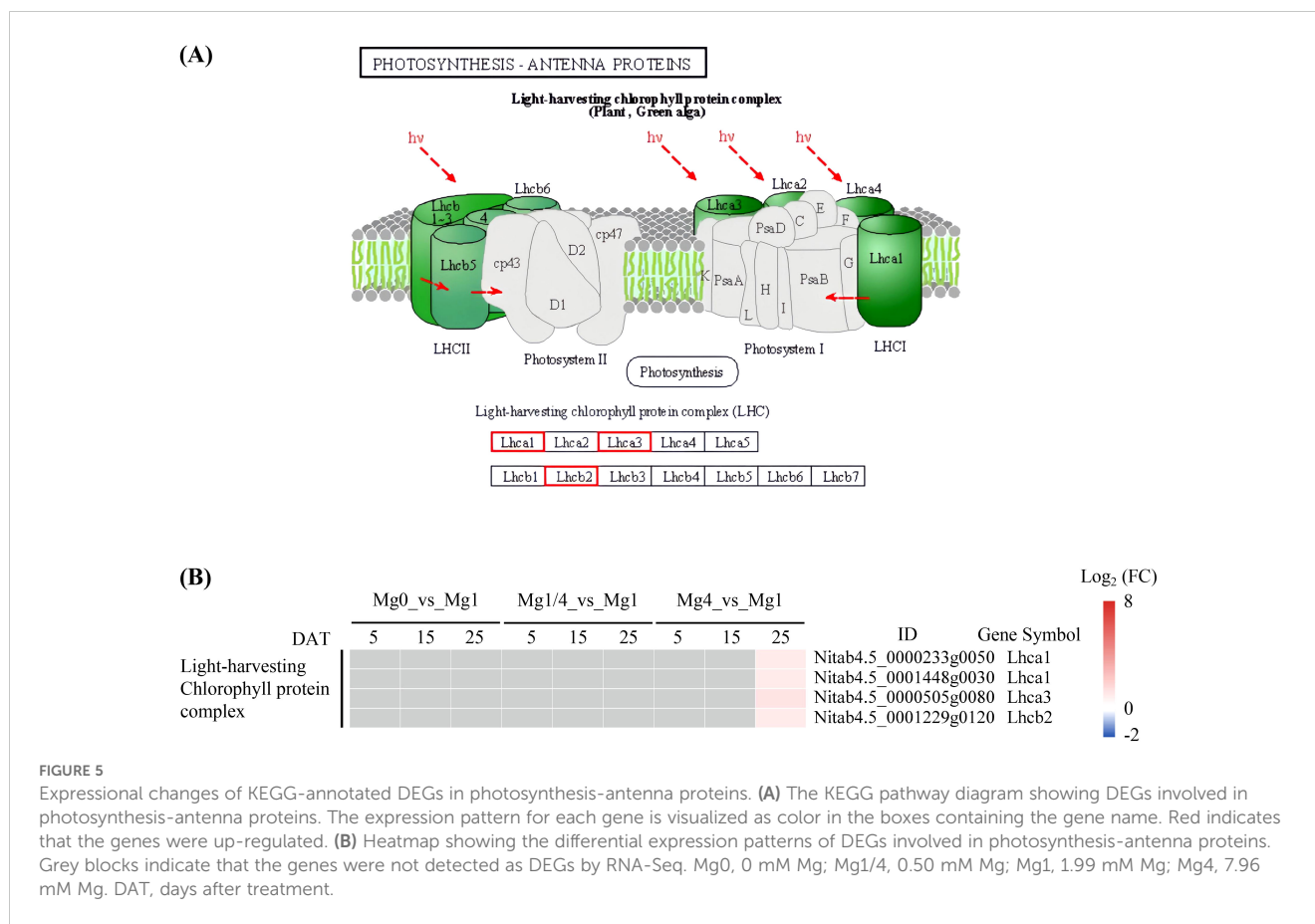
Expressional changes of DEGs involved in Mg distribution in tobacco in response to different Mg supplies. (A, B) Heatmap showing the differential expression patterns of two Mg<sup>2+</sup> transporters (MGTs) DEGs and one Mg<sup>2+</sup>/H<sup>+</sup> exchanger (MHX) DEG, respectively, at 5, 15, and 25 DAT. Grey blocks indicate that the genes were not detected as DEGs by RNA-Seq. Mg0, 0 mM Mg; Mg1/4, 0.50 mM Mg; Mg1, 1.99 mM Mg; Mg4, 7.96 mM Mg. DAT, days after treatment. (C–E) qRT-PCR validation of three DEGs *NtMGT7* (*Nitab4.5\_0003331g0150*), *NtMGT9* (*Nitab4.5\_0000436g0030*), and *NtMHX1* (*Nitab4.5\_0005805g0040*) in leaves of the Mg0, Mg1/4, Mg1, and Mg4 seedlings at 25 DAT. The tobacco *EF-1α* gene was used as an internal control. Significance levels \*p < 0.05, \*\*p < 0.01, ns, not significant. Different letters (a, b, c, d) above the columns indicate statistical differences (p < 0.05). (F) Subcellular localization of *NtMGT7* (*Nitab4.5\_0003331g0150*), *NtMGT9* (*Nitab4.5\_0000436g0030*), and *NtMHX1* (*Nitab4.5\_0005805g0040*) in *N. benthamiana* protoplasts. Scale bars = 10 μm. MGT7 (3331)-GFP, *NtMGT7* (*Nitab4.5\_0003331g0150*)-GFP fusion; MGT9 (0436)-GFP, *NtMGT9* (*Nitab4.5\_0000436g0030*)-GFP fusion; MHX1 (5805)-GFP, *NtMHX1* (*Nitab4.5\_0005805g0040*)-GFP fusion; ScCOX4-Red, mitochondria ScCOX4-DsRed marker; DsRed-OsTIP2, tonoplast Osy-TIP-DsRed marker.



**FIGURE 4** Expressional changes of KEGG-annotated DEGs in photosynthesis. **(A)** The KEGG pathway diagram showing DEGs involved in photosynthesis. The expression pattern for each gene is visualized as colors in the boxes containing the gene name. Red and green indicate that the genes were up-regulated and down-regulated, respectively. **(B)** Heatmap showing the differential expression patterns of DEGs involved in photosynthesis. Grey blocks indicate that the genes were not detected as DEGs by RNA-Seq. Mg0, 0 mM Mg; Mg1/4, 0.50 mM Mg; Mg1, 1.99 mM Mg; Mg4, 7.96 mM Mg. DAT, days after treatment.

to O<sub>2</sub>, resulting in the generation of O<sub>2</sub><sup>-</sup> and other reactive oxygen species (ROS) (Grossman and Takahashi, 2001). At 25 DAT, the root vitality (measured by the triphenylmethyl hydrazone (TTF) content), the relative level of CMP, H<sub>2</sub>O<sub>2</sub> content, and the activities of the enzymatic scavengers SOD, POD, and CAT in leaves of tobacco seedlings grown under different Mg levels were

measured. The root vitality was significantly lower in the Mg0 seedlings compared to that in the Mg1/4, Mg1, and Mg4 seedlings (Figure 7A), and the CMP level and H<sub>2</sub>O<sub>2</sub> content were notably higher in the Mg0 seedlings compared to the others (Figures 7B, C). These results indicate that Mg deficiency cause oxidative stress in tobacco seedlings. As for antioxidant enzymes,



the activity of SOD was significantly lower in the Mg0 seedlings compared to the Mg1 and Mg4 seedlings (Figure 7D). Similarly, CAT activity was notably lower in the Mg0 seedlings compared to the Mg1/4, Mg1, and Mg4 seedlings (Figure 7E). In contrast, POD activity in the Mg0 seedlings were significantly higher than that in the Mg1/4, Mg1, and Mg4 seedlings (Figure 7F).

We further characterized the DEGs related to antioxidant responses. Six SOD homologous genes were identified among the DEGs, including three copper/zinc superoxide dismutase genes (CSDs) and three iron superoxide dismutase genes (FSDs) (Figure 7G). Surprisingly, despite the lower SOD activity detected in the Mg0 seedlings at 25 DAT, all six SOD homologous genes were found to be up-regulated in the Mg0 seedlings at 15 DAT. Furthermore, one CAT2 homologous gene (*Nitab4.5\_0000588g0030*) was identified as a DEGs that was up-regulated in the Mg1/4 and Mg4 seedlings at 25 DAT (Figure 7G). Additionally, 10 POD homologous genes were identified among the DEGs, with the majority (seven out of 10) being up-regulated in the Mg0 seedlings at 25 DAT (Figure 7G), consistent with the significantly higher POD activity detected in the Mg0 seedlings at 25 DAT. Moreover, eight peroxiredoxin (*Prx*) homologous genes were identified among the DEGs, including three peroxiredoxin Q genes (*Prx Q*), two peroxiredoxin II E genes (*Prx II E*), and three 2-Cys peroxiredoxin B genes (2-Cys *Prx B*). All eight *Prx* homologous genes were up-regulated in the Mg0 seedlings at 15 DAT (Figure 7G). The transcriptional profiles of the DEGs *NitCSD2* (*Nitab4.5\_0004871g0010*) and *NitFSD3* (*Nitab4.5\_0000071g0190*) in the Mg0, Mg1/4, Mg1, and Mg4 seedlings at 15 DAT, and *NitPOD25*

(*Nitab4.5\_0003858g0010*) and *NitPOD52* (*Nitab4.5\_0002731g0010*) in the Mg0, Mg1/4, Mg1, and Mg4 seedlings at 25 DAT were validated using real-time RT-PCR. The results showed a significant up-regulation of these four genes in the Mg0 seedlings compared to the Mg1 seedlings, and the results were in line with the RNA-Seq data (Figures 7H-K). In addition to the SOD, CAT2, POD, and *Prx* homologous genes, a total of 44 glutathione S-transferase (GST) homologous genes were identified among the DEGs. These included three *NitGSTU7*, 21 *NitGSTU8*, three *NitGSTU9*, two *NitGSTU10*, six *NitGSTU19*, five *NitGSTU25*, two *NitGSTF8*, one *NitGSTF11*, and one *NitGSTL3* (Figure 8A). The majority of these GST homologous genes (39 out of 44) were up-regulated in the Mg0 seedlings at 15 and/or 25 DAT. The transcriptional profiles of the DEGs *NitGST8* (*Nitab4.5\_0000008g0130*), *NitGST8* (*Nitab4.5\_0017813g0010*), *NitGST10* (*Nitab4.5\_0000026g0030*), and *NitGSTF8* (*Nitab4.5\_0011583g0010*) in the Mg0, Mg1/4, Mg1, and Mg4 seedlings at 25 DAT were validated by real-time RT-PCR. The results showed a significant up-regulation of these four *NitGST* homologous genes in the Mg0 seedlings, consistent with the RNA-Seq data (Figures 8B-E).

## 4 Discussion

Mg is a vital element essential for plant growth and development. Both insufficient and excessive supply of Mg can adversely affect the growth, development, and productivity of various crops. In this study, we performed a comprehensive

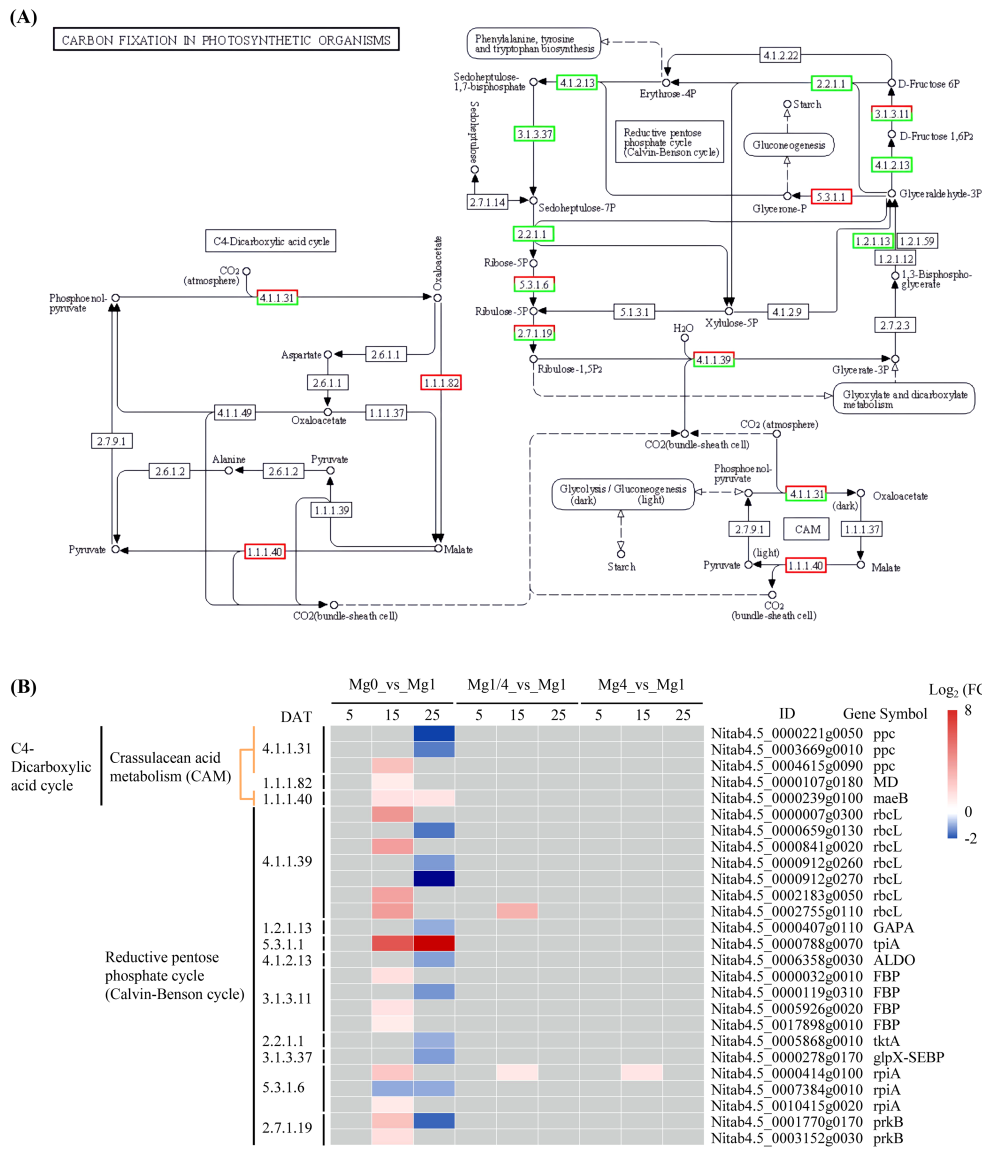


**FIGURE 6** Expressional changes of KEGG-annotated DEGs in carbon fixation in photosynthetic organisms. **(A)** The KEGG pathway diagram showing DEGs involved in carbon fixation in photosynthetic organisms. The expression pattern for each gene is visualized as colors in the boxes containing the gene name. Red and green indicate that the genes were up-regulated and down-regulated, respectively. **(B)** Heatmap showing the differential expression patterns of DEGs involved in carbon fixation in photosynthetic organisms. Grey blocks indicate that the genes were not detected as DEGs by RNA-Seq. Mg0, 0 mM Mg; Mg1/4, 0.50 mM Mg; Mg1, 1.99 mM Mg; Mg4, 7.96 mM Mg. DAT, days after treatment.

transcriptome analysis to explore the molecular responses of tobacco seedlings to varying levels of Mg supply. The analysis revealed significant changes in gene expression in tobacco leaves, particularly under conditions of Mg deficiency.

Plants have evolved strategies to regulate cellular Mg homeostasis. Studies on *Arabidopsis* and many other plants have revealed that MGTs and MHXs are crucial for uptake and distribution of Mg. In *Arabidopsis*, AtMGT1 and AtMGT10 have been demonstrated to be capable of transporting Mg<sup>2+</sup> (Li et al., 2001). AtMGT1 and AtMGT2 are localized in the tonoplast and facilitate mobilizing Mg<sup>2+</sup> into vacuole (Tang et al., 2022). AtMGT3 has been identified as being involved in regulating Mg homeostasis in mesophyll cells (Alexandersson et al., 2004; Whiteman et al., 2008). AtMGT5 is

localized in the mitochondria and functions as a Mg-importer at low micromolar levels while facilitating Mg efflux at higher millimolar concentrations (Li et al., 2008). AtMGT6 and AtMGT7 are also involved in regulating cellular Mg<sup>2+</sup> homeostasis. The mutation or knockdown of *AtMGT6* and/or *AtMGT7* result in Mg<sup>2+</sup> hypersensitivity (Gebert et al., 2009; Mao et al., 2014; Oda et al., 2016). MGTs are present in the plasma membrane, mitochondria, tonoplast, endoplasmic reticulum, and chloroplast (Oda et al., 2016), indicating their role in mediating Mg movement between the cytosol and organelles. In this study, two homologous MGTs were identified as DEGs, including *NtMGT7* and *NtMGT9*. These two genes were down-regulated in tobacco seedlings under Mg deficiency at 25 DAT (Figure 3A). While many MGTs were identified

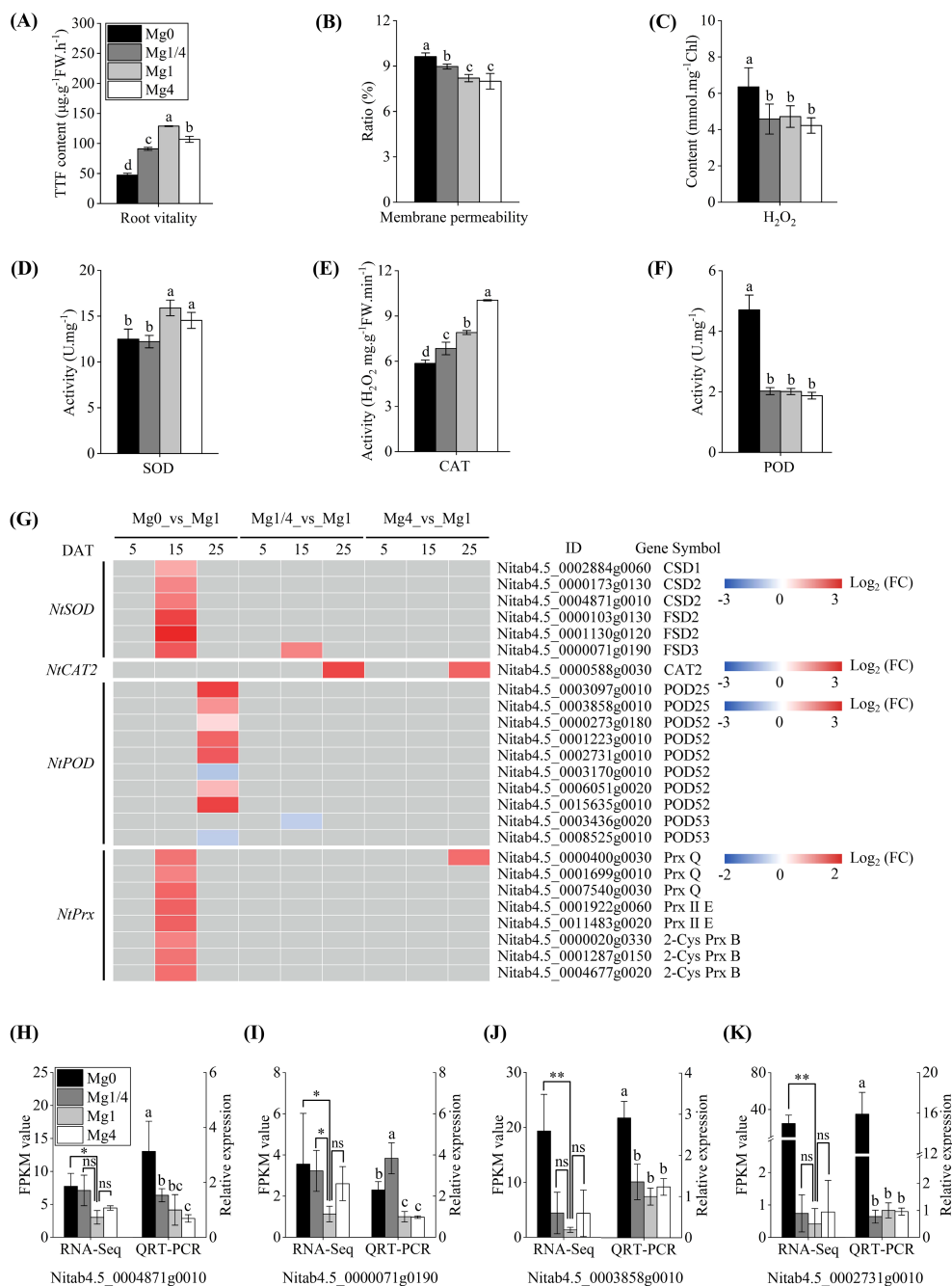


**FIGURE 7** Effects of different Mg supplies on physiological parameters related to antioxidant defense and expression changes of key DEGs involved in enzymatic scavenging. **(A–C)** Root vitality, Cell membrane permeability, and hydrogen peroxide (H<sub>2</sub>O<sub>2</sub>) content, in leaves of tobacco seedlings grown under different Mg supplies at 25 DAT. **(D–F)** Activities of superoxide dismutase (SOD), catalase (CAT), and peroxidase (POD) in leaves of tobacco seedlings grown under different Mg supplies at 25 DAT. **(G)** Heatmap showing the differential expression levels of SOD, CAT2, POD, and peroxiredoxin (Prx) family DEGs, respectively. Grey blocks indicate that the genes were not detected as DEGs by RNA-Seq. **(H–K)** qRT-PCR validation of two DEGs *NtCSD2* (*Nitab4.5\_0004871g0010*) and *NtFSD3* (*Nitab4.5\_0000071g0190*) in the Mg0, Mg1/4, Mg1, and Mg4 seedlings at 15 DAT, and two DEGs *NtPOD25* (*Nitab4.5\_0003858g0010*) and *NtPOD52* (*Nitab4.5\_0002731g0010*) in the Mg0, Mg1/4, Mg1, and Mg4 seedlings at 25 DAT. The tobacco *EF-1α* gene was used as an internal control. Mg0, 0 mM Mg; Mg1/4, 0.50 mM Mg; Mg1, 1.99 mM Mg; Mg4, 7.96 mM Mg. DAT, days after treatment. Significance levels \**p* < 0.05, \*\**p* < 0.01, ns, not significant. Different letters (a, b, c, d) above the columns indicate statistical differences (*p* < 0.05).

that are up-regulated in plants under Mg starvation in previous studies (Hermans et al., 2010; Mao et al., 2014; Li et al., 2016; Ge et al., 2022; Bin et al., 2023), our study did not find significantly up-regulated homologous *MGTs* in the Mg0 seedlings. This could be due to using

only leaves for RNA-Seq analysis in the present study. Our research further demonstrated that the homologous *NtMGT7* and *NtMGT9* are localized in the mitochondria (Figure 3F), suggesting their involvement in Mg transport between the cytosol and mitochondria. *MHX*

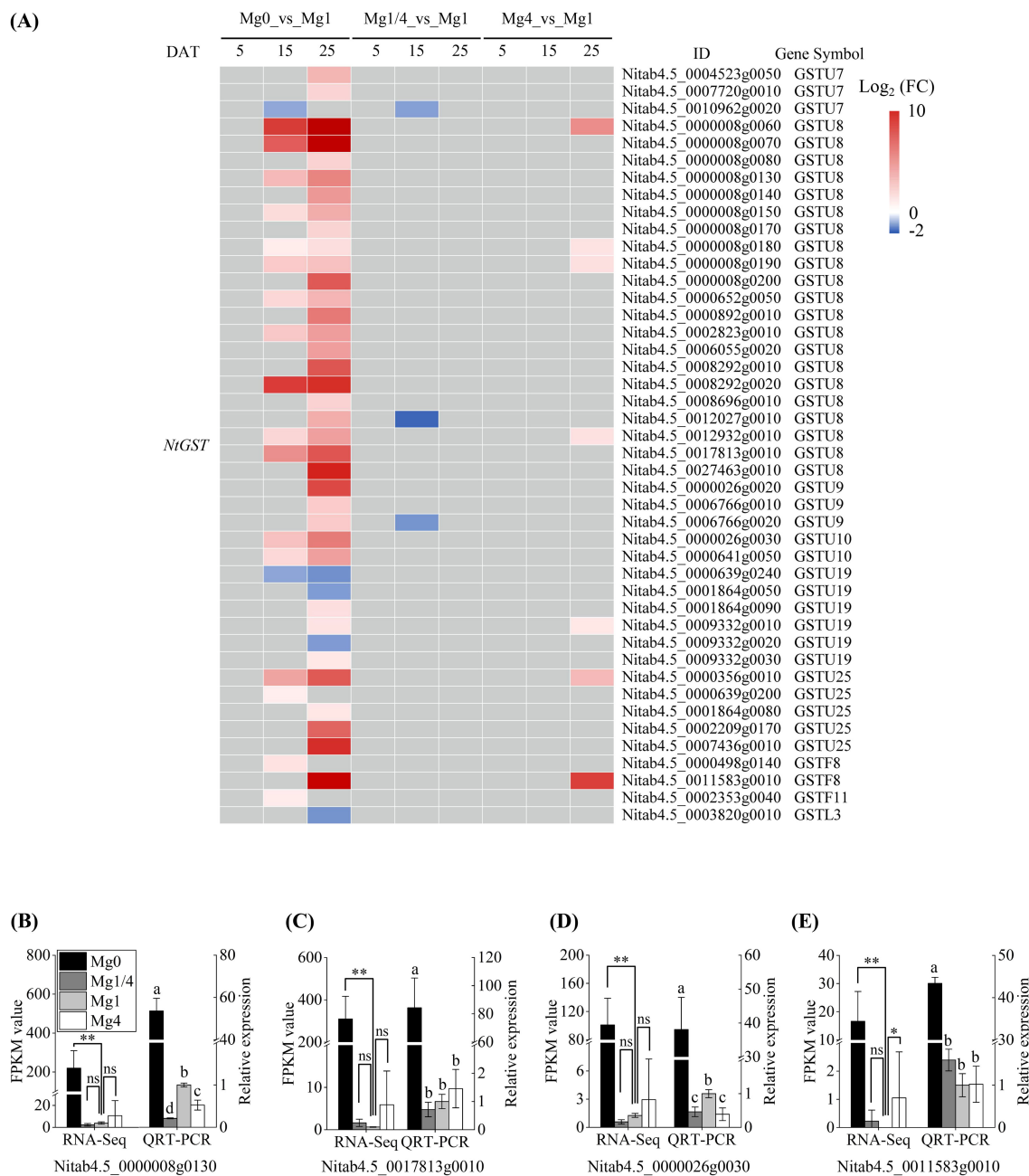


FIGURE 8

Expressional changes of glutathione S-transferase (GST) family DEGs. **(A)** Heatmap showing the differential expression levels of GST family DEGs in leaves of tobacco seedlings grown under different Mg supplies. Grey blocks indicate that the genes were not detected as DEGs by RNA-Seq. **(B-E)** qRT-PCR validation of four DEGs *NtGST8* (*Nitab4.5\_0000008g0130*), *NtGST8* (*Nitab4.5\_0017813g0010*), *NtGST10* (*Nitab4.5\_0000026g0030*), and *NtGSTF8* (*Nitab4.5\_0011583g0010*) in the Mg0, Mg1/4, Mg1, and Mg4 seedlings at 25 DAT. The tobacco *EF-1α* gene was used as an internal control. DAT, days after treatment. Significance levels \* $p < 0.05$ , \*\* $p < 0.01$ , ns, not significant. Different letters (a, b, c, d) above the columns indicate statistical differences ( $p < 0.05$ ).

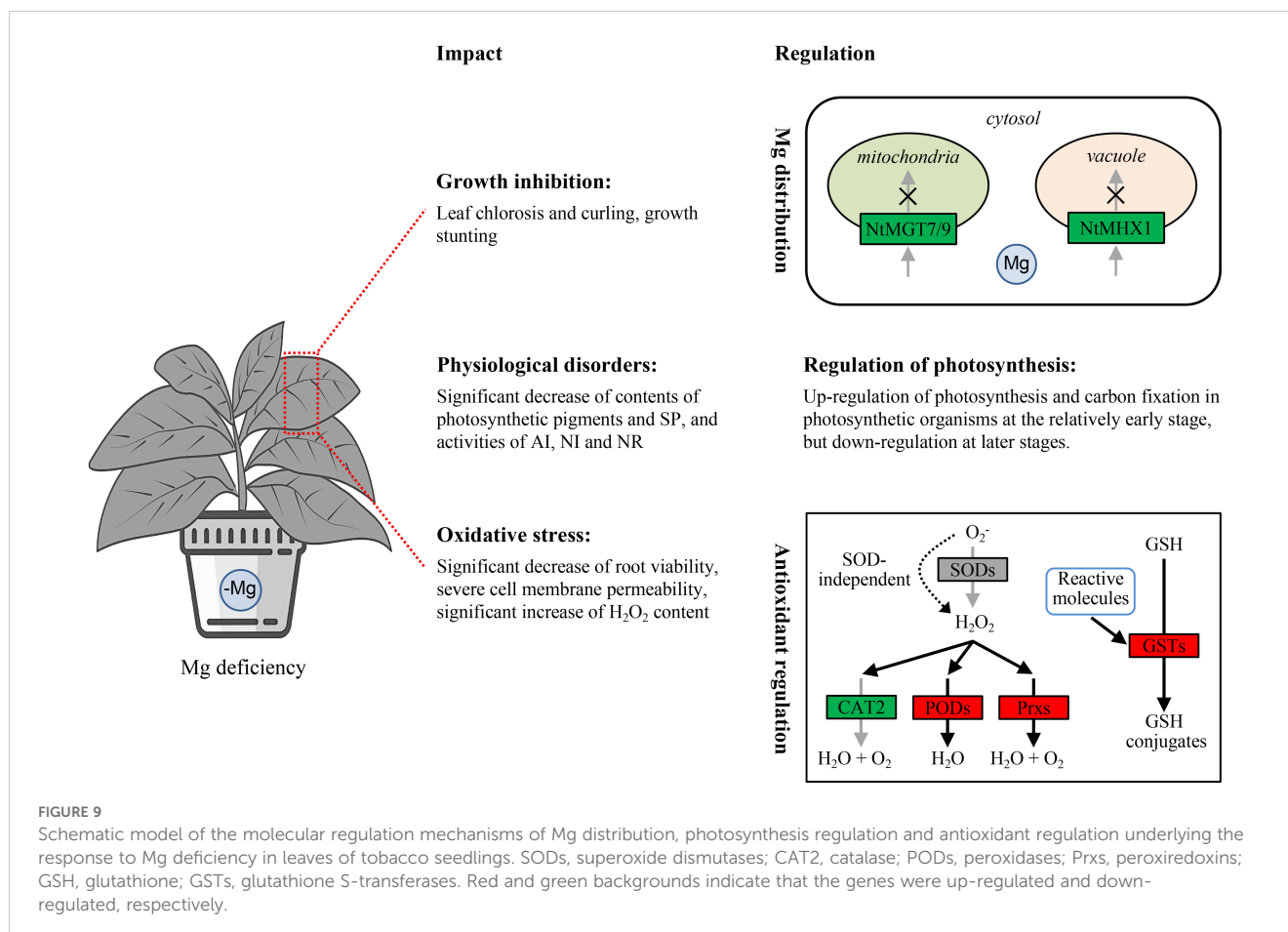
functions as a proton exchanger responsible for  $Mg^{2+}$  transport across the vacuolar membrane (Berezin et al., 2008; Kobayashi, 2022). In the present study, a homologous *NtMHX1* gene was identified as a DEG. Similar to *NtMGT7* and *NtMGT9*, *NtMHX1* was down-regulated in tobacco seedlings under Mg deficiency at 25 DAT (Figure 3B). Consistent with the localization of *AtMHX1* in the vacuole membrane of *Arabidopsis* cells (Conn et al., 2011), the homologous *NtMHX1* is localized in the vacuole membrane of *N. benthamiana* cells

(Figure 3F). Overall, these results suggest a down-regulation of Mg-trafficking from the cytosol to mitochondria and vacuole in the leaf cells of tobacco seedlings experiencing Mg deficiency (Figure 9).

It is widely acknowledged that Mg deficiency inhibits photosynthesis in various plant species, such as Citrus (Yang et al., 2012), watermelon (Huang et al., 2016), barley (Jaghdani et al., 2021a), *Spinacia oleracea* (Jaghdani et al., 2021b), cucumber (Meng et al., 2023), and rice (Zhou et al., 2024). Mg is essential for

chlorophyll formation. In the present study, significantly lower levels of Chla and Chlb were observed in the Mg0 seedlings compared to those supplied with varying levels of Mg (Mg1/4, Mg1, and Mg4), indicating a decline of chlorophyll formation caused by Mg deficiency. KEGG analysis revealed that the pathways of photosynthesis and carbon fixation in photosynthetic organisms were significantly enriched among the up-regulated DEGs in the Mg0 seedlings at 15 DAT, but among the down-regulated DEGs in the Mg0 seedlings at 25 DAT (Figures 4B, 6B). A total of 45 DEGs related to PSII, PSI, photosynthetic electron transport, and F-type ATPase were identified, with 32 being up-regulated in the Mg0 seedlings at 15 DAT, and nine down-regulated in the Mg0 seedlings at 25 DAT (Figure 4B); furthermore, a total of 26 DEGs related to C4-Dicarboxylic acid cycle and reductive pentose phosphate cycle were identified, with 15 up-regulated in the Mg0 seedlings at 15 DAT, and 12 down-regulated in the Mg0 seedlings at 25 DAT (Figures 6A, B). These results suggest that Mg deficiency initially triggers the up-regulated expression of genes related to photosynthesis and carbon fixation in tobacco seedlings at relatively earlier stages, followed by down-regulation at later stages (Figure 9). The down-regulation of genes related to photosynthesis and carbon fixation at relatively late stages aligns with previous findings showing that Mg deficiency inhibits plant photosynthesis (Yang et al., 2012; Huang et al., 2016; Jaghdani et al., 2021a; b; Meng et al., 2023; Zhou et al., 2024).

Deficiencies in macronutrient or micronutrient elements can lead to oxidative stress in plants. For example, Zn deficiency can cause severe cell membrane damage and increased  $H_2O_2$  levels in tobacco seedlings (Lu et al., 2023). Similarly, Mg deficiency can impair the electron transport rate, leading to an over-reduction of the electron transport chain, ultimately triggering the production of ROS (Hermans and Verbruggen, 2005; Tang et al., 2012). In the present study, it was observed that root vitality was significantly reduced, and the levels of cell membrane damage (as indicated by CMP) and  $H_2O_2$  were significantly higher in leaves of tobacco seedlings experiencing Mg deficiency (Figures 7A-C), indicating the induction of oxidative stress (Figures 7A-C). Six *NtSOD* family DEGs were up-regulated in the Mg0 seedlings at 15 DAT (Figure 7G). Conversely, reduced SOD activity was observed in tobacco seedlings under Mg starvation at 25 DAT (Figure 7D). This reduction in SOD activity could be due to metabolic disorders caused by Mg deficiency or other unknown reasons. Additionally, the finding suggests the potential dismutation of oxide ion ( $O_2^-$ ) through an SOD-independent mechanism in tobacco seedlings under Mg deficiency (Figure 9). Similarly, decreased CAT activity was observed in tobacco seedlings experiencing Mg starvation at 25 DAT (Figure 7E). In contrast, significantly enhanced POD activity was detected in the Mg0 seedlings at 25 DAT (Figure 7F). Consistent with this increased activity, seven *NtPOD* homologous genes were up-regulated in leaves of tobacco seedlings under Mg



deficiency (Figure 7G). Moreover, eight DEGs encoding Prxs, a specific class of H<sub>2</sub>O<sub>2</sub>-decomposing antioxidant enzymes (Smirnoff and Arnaud, 2019), were up-regulated in the Mg<sup>0</sup> seedlings at 15 DAT (Figure 7G). The up-regulation of these *NtPODs* and *NtPrxs* DEGs is expected to facilitate ROS scavenging (Figure 9). Furthermore, a total of 44 *NtGST* homologous genes were identified as DEGs, with 39 out of the 44 *NtGST* DEGs being up-regulated in response to Mg deficiency at 15 and/or 25 DAT (Figure 8A). Similarly, the up-regulation of *NtGSTs* would contribute to maintaining ROS homeostasis (Figure 9).

## 5 Conclusions

Our results demonstrated that Mg deficiency caused severe physiological disorders and inhibits the growth of tobacco seedlings. The global gene expression profiles revealed potential mechanisms involved in the response to Mg deficiency in tobacco leaves. These mechanisms include the down-regulation of genes associated with Mg trafficking from the cytosol to mitochondria and vacuoles, the down-regulation of genes related to photosynthesis and carbon fixation at later stages, and the up-regulation of genes related to antioxidant defenses.

## Data availability statement

The datasets presented in this study can be found in online repositories. The names of the repository/repositories and accession number(s) can be found in the article/Supplementary Material.

## Author contributions

TL: Data curation, Investigation, Methodology, Software, Writing – original draft. JLi: Data curation, Investigation, Methodology, Software, Writing – review & editing. SW: Investigation, Methodology, Writing – review & editing. RY: Data curation, Methodology, Writing – review & editing. MQ: Data curation, Methodology, Writing – review & editing. RX: Data curation, Investigation, Writing – review & editing. YL: Data curation, Investigation, Writing – review & editing. JG: Data curation, Investigation, Writing – review & editing. YW: Data curation, Methodology, Writing – review & editing. YK: Data curation, Methodology, Writing – review & editing. CL: Project administration, Supervision, Writing – review & editing. JG: Project administration, Supervision, Writing – review & editing. JLu: Formal analysis, Supervision, Writing – review & editing. WT: Formal

analysis, Supervision, Writing – review & editing. SC: Conceptualization, Project administration, Resources, Software, Supervision, Writing – original draft, Writing – review & editing. WL: Conceptualization, Project administration, Resources, Supervision, Writing – review & editing.

## Funding

The author(s) declare financial support was received for the research, authorship, and/or publication of this article. This work was funded by the Research Foundation of Fujian Provincial Tobacco Monopoly Bureau (2019350000240145; 2019350000240009).

## Conflict of interest

The authors declare that the research was conducted in the absence of any commercial or financial relationships that could be construed as a potential conflict of interest.

## Publisher's note

All claims expressed in this article are solely those of the authors and do not necessarily represent those of their affiliated organizations, or those of the publisher, the editors and the reviewers. Any product that may be evaluated in this article, or claim that may be made by its manufacturer, is not guaranteed or endorsed by the publisher.

## Supplementary material

The Supplementary Material for this article can be found online at: <https://www.frontiersin.org/articles/10.3389/fpls.2024.1483217/full#supplementary-material>

SUPPLEMENTARY TABLE 1  
Primers used in this study.

SUPPLEMENTARY TABLE 2  
Total DEGs in Mg<sup>0</sup>, Mg<sup>1/4</sup>, and Mg<sup>4</sup> in comparison to Mg<sup>1</sup>.

SUPPLEMENTARY TABLE 3  
DEGs in Mg<sup>0</sup>, Mg<sup>1/4</sup>, and Mg<sup>4</sup> in comparison to Mg<sup>1</sup> at 5, 15, and 25 DAT, respectively.

SUPPLEMENTARY TABLE 4  
Significant KEGG pathways of DEGs in Mg<sup>0</sup>, Mg<sup>1/4</sup>, and Mg<sup>4</sup> in comparison to Mg<sup>1</sup>.

## References

Alexandersson, E., Saalbach, G., Larsson, C., and Kjellbom, P. (2004). Arabidopsis plasma membrane proteomics identifies components of transport, signal transduction and membrane trafficking. *Plant Cell Physiol.* 45, 1543–1556. doi: 10.1093/pcp/pch209

Anderson, M. D., Prasad, T. K., and Stewart, C. R. (1995). Changes in isozyme profiles of catalase, peroxidase, and glutathione reductase during acclimation to chilling in mesocotyls of maize seedlings. *Plant Physiol.* 109, 1247–1257. doi: 10.1104/pp.109.4.1247

- Berezin, I., Mizrachy-Dagry, T., Brook, E., Mizrahi, K., Elazar, M., Zhuo, S., et al. (2008). Overexpression of AtMHX in tobacco causes increased sensitivity to  $Mg^{2+}$ ,  $Zn^{2+}$ , and  $Cd^{2+}$  ions, induction of V-ATPase expression, and a reduction in plant size. *Plant Cell Rep.* 27, 939–949. doi: 10.1007/s00299-007-0502-9
- Bin, M., Yi, G., and Zhang, X. (2023). Discovery and characterization of magnesium transporter (MGT) gene family in *Citrus sinensis* and their role in magnesium deficiency stress. *Plant Growth Regulation.* 100, 733–746. doi: 10.21203/rs.3.rs-2296447/v1
- Cakmak, I. (2013). Magnesium in crop production, food quality and human health. *Plant Soil.* 368, 1–4. doi: 10.1007/s11104-013-1781-2
- Cakmak, I., and Kirkby, E. A. (2008). Role of magnesium in carbon partitioning and alleviating photooxidative damage. *Physiol. Plant.* 133, 692–704. doi: 10.1111/j.1399-3054.2007.01042.x
- Chaudhry, A. H., Nayab, S., Hussain, S. B., Ali, M., and Pan, Z. (2021). Current understandings on magnesium deficiency and future outlooks for sustainable agriculture. *Int. J. Mol. Sci.* 22, 1819. doi: 10.3390/ijms22041819
- Chen, Z., Zheng, W., Chen, L., Li, C., Liang, T., Chen, Z., et al. (2019). Green fluorescent protein- and *Discosoma* sp. red fluorescent protein-tagged organelle marker lines for protein subcellular localization in rice. *Front. Plant Sci.* 10. doi: 10.3389/fpls.2019.01421
- Clemensson-Lindell, A. (1994). Triphenyltetrazolium chloride as an indicator of fine-root vitality and environmental stress in coniferous forest stands: applications and limitations. *Plant Soil.* 159, 297–300. doi: 10.1007/bf00009293
- Conn, S. J., Conn, V., Tyerman, S. D., Kaiser, B. N., Leigh, R. A., and Gilliam, M. (2011). Magnesium transporters, MGT2/MRS2-1 and MGT3/MRS2-5, are important for magnesium partitioning within *Arabidopsis thaliana* mesophyll vacuoles. *New Phytol.* 190 (3), 583–594. doi: 10.1111/j.1469-8137.2010.03619.x
- Cowan, J. A. (2002). Structural and catalytic chemistry of magnesium-dependent enzymes. *Biometals* 15, 225–235. doi: 10.1023/a:1016022730880
- Deng, N., Zhu, H., Xiong, J., Gong, S., Xie, K., Shang, Q., et al. (2023). Magnesium deficiency stress in rice can be alleviated by partial nitrate nutrition supply. *Plant Physiol. Biochem.* 196, 463–471. doi: 10.1016/j.plaphy.2023.02.005
- Ge, M., Zhong, R., Sadeghnezhad, E., Hakeem, A., Xiao, X., Wang, P., et al. (2022). Genome-wide identification and expression analysis of magnesium transporter gene family in grape (*Vitis vinifera*). *BMC Plant Biol.* 22, 217. doi: 10.1186/s12870-022-03599-5
- Gebert, M., Meschenmoser, K., Svidova, S., Weghuber, J., Schweyen, R., Eifler, K., et al. (2009). A root-expressed magnesium transporter of the MRS2/MGT gene family in *Arabidopsis thaliana* allows for growth in low- $Mg^{2+}$  environments. *Plant Cell.* 21, 4018–4030. doi: 10.1105/tpc.109.070557
- Grossman, A., and Takahashi, H. (2001). Macronutrient utilization by photosynthetic eukaryotes and the fabric of interactions. *Annu. Rev. Plant Biol.* 52, 163–210. doi: 10.1146/annurev.arplant.52.1.163
- Hauer-Jákl, M., and Tränkner, M. (2019). Critical leaf magnesium thresholds and the impact of magnesium on plant growth and photo-oxidative defense: a systematic review and meta-analysis from 70 years of research. *Front. Plant Sci.* 10. doi: 10.3389/fpls.2019.00766
- Hermans, C., and Verbruggen, N. (2005). Physiological characterization of Mg deficiency in *Arabidopsis thaliana*. *J. Exp. Bot.* 56, 2153–2161. doi: 10.1093/jxb/eri215
- Hermans, C., Vuylsteke, M., Coppens, F., Craciun, A., Inzé, D., and Verbruggen, N. (2010). Early transcriptomic changes induced by magnesium deficiency in *Arabidopsis thaliana* reveal the alteration of circadian clock gene expression in roots and the triggering of abscisic acid-responsive genes. *New Phytol.* 187, 119–131. doi: 10.1111/j.1469-8137.2010.03258.x
- Huang, Y., Jiao, Y., Nawaz, M. A., Chen, C., Liu, L., Lu, Z., et al. (2016). Improving magnesium uptake, photosynthesis and antioxidant enzyme activities of watermelon by grafting onto pumpkin rootstock under low magnesium. *Plant Soil.* 409, 229–246. doi: 10.1007/s11104-016-2965-3
- Ishfaq, M., Wang, Y., Yan, M., Wang, Z., Wu, L., Li, C., et al. (2022). Physiological essence of magnesium in plants and its widespread deficiency in the farming system of China. *Front. Plant Sci.* 13. doi: 10.3389/fpls.2022.802274
- Jaghdani, S. J., Jahns, P., and Tränkner, M. (2021a). Mg deficiency induces photo-oxidative stress primarily by limiting  $CO_2$  assimilation and not by limiting photosynthetic light utilization. *Plant Sci.* 302, 110751. doi: 10.1016/j.plantsci.2020.110751
- Jaghdani, S. J., Jahns, P., and Tränkner, M. (2021b). The impact of magnesium deficiency on photosynthesis and photoprotection in *Spinacia oleracea*. *Plant Stress.* 2, 100040. doi: 10.1016/j.stress.2021.100040
- Kim, D., Langmead, B., and Salzberg, S. L. (2015). HISAT: a fast spliced aligner with low memory requirements. *Nat. Methods* 12, 357–360. doi: 10.1038/nmeth.3317
- Kobayashi, N. I. (2022). “An introduction to the  $Mg^{2+}$  transporters in plants,” in *Cation transporters in plants* (Academic Press), 129–146. doi: 10.1016/B978-0-323-85790-1.00024-5
- Leech, R. M., Leese, B. M., and Jellings, A. J. (1985). Variation in cellular ribulose-1, 5-bisphosphate-carboxylase content in leaves of Triticum genotypes at three levels of ploidy. *Planta* 166, 259–263. doi: 10.1007/bf00397357
- Li, H., Du, H., Huang, K., Chen, X., Liu, T., Gao, S., et al. (2016). Identification, and functional and expression analyses of the CorA/MRS2/MGT-type magnesium transporter family in maize. *Plant Cell Physiol.* 57, 1153–1168. doi: 10.1093/pcp/pcw064
- Li, J., Muneer, M. A., Sun, A., Guo, Q., Wang, Y., Huang, Z., et al. (2023). Magnesium application improves the morphology, nutrients uptake, photosynthetic traits, and quality of tobacco (*Nicotiana tabacum* L.) under cold stress. *Front. Plant Sci.* 14. doi: 10.3389/fpls.2023.1078128
- Li, L., Tutone, A. F., Drummond, R. S., Gardner, R. C., and Luan, S. (2001). A novel family of magnesium transport genes in *Arabidopsis*. *Plant Cell.* 13, 2761–2775. doi: 10.1105/tpc.010352
- Li, L. G., Sokolov, L. N., Yang, Y. H., Li, D. P., Ting, J., Pandey, G. K., et al. (2008). A mitochondrial magnesium transporter functions in *Arabidopsis* pollen development. *Mol. Plant* 1, 675–685. doi: 10.1093/mp/ssn031
- Li, W., Zheng, C., Ke, Y., Chen, S., Guo, J., and Li, C. (2022). Effects of magnesium fertilizer application on soil magnesium supply and growth and development, yield and quality of flue-cured tobacco. *J. Agricult.* 12, 33–40. doi: 10.11923/j.issn.2095-4050.cjas2020-0217
- Lichtenthaler, H. K., and Buschmann, C. (2001). Chlorophylls and carotenoids: Measurement and characterization by UV-VIS spectroscopy. *Curr. Protoc. Food Analytical. Chem.* 1, F4.3.1–F4.3.8. doi: 10.1002/0471142913.faf0403s01
- Liu, G., Fu, Y., Liu, Q., Sun, X., Wang, H., and Zhang, H. (1998). Effects of magnesium level on the growth, yield and quality of flue-cured tobacco. *Acta Agricult. Universitatis Henanensis.* 32, 34–37. doi: 10.16445/j.cnki.1000-2340.1998.s1.007
- Livak, K. J., and Schmittgen, T. D. (2001). Analysis of relative gene expression data using real-time quantitative PCR and the  $2^{-\Delta\Delta CT}$  method. *Methods* 25, 402–408. doi: 10.1006/meth.2001.1262
- Love, M. I., Huber, W., and Anders, S. (2014). Moderated estimation of fold change and dispersion for RNA-seq data with DESeq2. *Genome Biol.* 15, 1–21. doi: 10.1186/s13059-014-0550-8
- Lu, J., Ye, R., Qu, M., Wang, Y., Liang, T., Lin, J., et al. (2023). Combined transcriptome and proteome analysis revealed the molecular regulation mechanisms of zinc homeostasis and antioxidant machinery in tobacco in response to different zinc supplies. *Plant Physiol. Biochem.* 202, 107919. doi: 10.1016/j.plaphy.2023.107919
- Maathuis, F. J. (2009). Physiological functions of mineral macronutrients. *Curr. Opin. Plant Biol.* 12, 250–258. doi: 10.1016/j.pbi.2009.04.003
- Mao, D., Chen, J., Tian, L., Liu, Z., Yang, L., Tang, R., et al. (2014). Arabidopsis transporter MGT6 mediates magnesium uptake and is required for growth under magnesium limitation. *Plant Cell.* 26, 2234–2248. doi: 10.1105/tpc.114.124628
- Marschner, H., and Cakmak, I. (1989). High light intensity enhances chlorosis and necrosis in leaves of zinc, potassium, and magnesium deficient bean (*Phaseolus vulgaris*) plants. *J. Plant Physiol.* 134, 308–315. doi: 10.1016/S0176-1617(89)80248-2
- Meng, X., Bai, S., Wang, S., Pan, Y., Chen, K., Xie, K., et al. (2023). The sensitivity of photosynthesis to magnesium deficiency differs between rice (*Oryza sativa* L.) and cucumber (*Cucumis sativus* L.). *Front. Plant Sci.* 14. doi: 10.3389/fpls.2023.1164866
- Moss, G. I., and Higgins, M. L. (1974). Magnesium influences on the fruit quality of sweet orange (*Citrus sinensis* L. Osbeck). *Plant Soil.* 41, 103–112. doi: 10.1007/BF00017948
- Musharraf, S. G., Shoaib, M., Siddiqui, A. J., Najam-ul-Haq, M., and Ahmed, A. (2012). Quantitative analysis of some important metals and metalloids in tobacco products by inductively coupled plasma-mass spectrometry (ICP-MS). *Chem. Cent. J.* 6, 1–12. doi: 10.1186/1752-153X-6-56
- Oda, K., Kamiya, T., Shikanai, Y., Shigenobu, S., Yamaguchi, K., and Fujiwara, T. (2016). The Arabidopsis Mg transporter, MRS2-4, is essential for Mg homeostasis under both low and high Mg conditions. *Plant Cell Physiol.* 57, 754–763. doi: 10.1093/pcp/pcv196
- Palta, J. P., and Stadelmann, E. J. (1997). Effect of turgor pressure on water permeability of *Allium cepa* epidermis cell membranes. *J. Membrane Biol.* 33, 231–247. doi: 10.1007/bf01869518
- Qu, M., Zhang, Z., Liang, T., Niu, P., Wu, M., Chi, W., et al. (2021). Overexpression of a methyl-CpG-binding protein gene *OsMBD707* leads to larger tiller angles and reduced photoperiod sensitivity in rice. *BMC Plant Biol.* 21, 100. doi: 10.21203/rs.3.rs-95600/v1
- Schmidt, G. W., and Delaney, S. K. (2010). Stable internal reference genes for normalization of real-time RT-PCR in tobacco (*Nicotiana tabacum*) during development and abiotic stress. *Mol. Genet. Genomics* 283, 233–241. doi: 10.1007/s00438-010-0511-1
- Senbayram, M., Gransee, A., Wahle, V., and Thiel, H. (2015). Role of magnesium fertilizers in agriculture: Plant-soil continuum. *Crop Pasture Sci.* 66, 1219–1229. doi: 10.1071/CP15104
- Shaul, O. (2002). Magnesium transport and function in plants: the tip of the iceberg. *Biometals* 15, 309–323. doi: 10.1023/A:1016091118585
- Shaul, O., Hilgemann, D. W., de-Almeida-Engler, J., Van Montagu, M., Inzé, D., and Galili, G. (1999). Cloning and characterization of a novel  $Mg^{2+}/H^+$  exchanger. *EMBO J.* 18, 3973–3980. doi: 10.1093/emboj/18.14.3973
- Smirnov, N., and Arnaud, D. (2019). Hydrogen peroxide metabolism and functions in plants. *New Phytol.* 221, 1197–1214. doi: 10.1111/nph.15488
- Tang, N., Li, Y., and Chen, L. S. (2012). Magnesium deficiency-induced impairment of photosynthesis in leaves of fruiting *Citrus reticulata* trees accompanied by up-

- regulation of antioxidant metabolism to avoid photo-oxidative damage. *J. Plant Nutr. Soil Sci.* 175, 784–793. doi: 10.1002/jpln.201100329
- Tang, R. J., and Luan, S. (2017). Regulation of calcium and magnesium homeostasis in plants: from transporters to signaling network. *Curr. Opin. Plant Biol.* 39, 97–105. doi: 10.1016/j.pbi.2017.06.009
- Tang, R. J., Yang, Y., Yan, Y. W., Mao, D. D., Yuan, H. M., Wang, C., et al. (2022). Two transporters mobilize magnesium from vacuolar stores to enable plant acclimation to magnesium deficiency. *Plant Physiol.* 190, 1307–1320. doi: 10.1093/plphys/kiac330
- Trapnell, C., Williams, B. A., Pertea, G., Mortazavi, A., Kwan, G., Van Baren, M. J., et al. (2010). Transcript assembly and quantification by RNA-Seq reveals unannotated transcripts and isoform switching during cell differentiation. *Nat. Biotechnol.* 28, 511–515. doi: 10.1038/nbt.1621
- Verbruggen, N., and Hermans, C. (2013). Physiological and molecular responses to magnesium nutritional imbalance in plants. *Plant Soil.* 368, 87–99. doi: 10.1007/s11104-013-1589-0
- Wang, Y., Zhang, X., Zhang, W., Peng, M., Tan, G., Qaseem, M. F., et al. (2023). Physiological and transcriptomic responses to magnesium deficiency in *Neolamarckia Cadamba*. *Plant Physiol. Biochem.* 197, 107645. doi: 10.1016/j.plaphy.2023.107645
- Whiteman, S. A., Serazetdinova, L., Jones, A. M., Sanders, D., Rathjen, J., Peck, S. C., et al. (2008). Identification of novel proteins and phosphorylation sites in a tonoplast enriched membrane fraction of *Arabidopsis thaliana*. *Proteomics* 8, 3536–3547. doi: 10.1002/pmic.200701104
- Xie, C., Mao, X., Huang, J., Ding, Y., Wu, J., Dong, S., et al. (2011). KOBAS 2.0: a web server for annotation and identification of enriched pathways and diseases. *Nucleic Acids Res.* 39, W316–W322. doi: 10.1093/nar/gkr483
- Xu, Q., Chen, A., Dai, P., Zheng, G., and Chen, Z. (2011). Effects of rational application of magnesium fertilizers on growth, yield and quality of flue-cured tobacco. *Chin. Tobacco Sci.* 32, 33–36. doi: 10.3969/j.issn.1007-5119.2011.02.008
- Yan, Y. W., Mao, D. D., Yang, L., Qi, J. L., Zhang, X. X., Tang, Q. L., et al. (2018). Magnesium transporter MGT6 plays an essential role in maintaining magnesium homeostasis and regulating high magnesium tolerance in *Arabidopsis*. *Front. Plant Sci.* 9. doi: 10.3389/fpls.2018.00274
- Yang, G. H., Yang, L. T., Jiang, H. X., Li, Y., Wang, P., and Chen, L. S. (2012). Physiological impacts of magnesium-deficiency in Citrus seedlings: photosynthesis, antioxidant system and carbohydrates. *Trees* 26, 1237–1250. doi: 10.1007/s00468-012-0699-2
- Young, M. D., Wakefield, M. J., Smyth, G. K., and Oshlack, A. (2010). Gene ontology analysis for RNA-seq: accounting for selection bias. *Genome Biol.* 11, R14. doi: 10.1186/gb-2010-11-2-r14
- Zhou, H., Peng, J., Zhao, W., Zeng, Y., Xie, K., and Huang, G. (2024). Leaf diffusional capacity largely contributes to the reduced photosynthesis in rice plants under magnesium deficiency. *Plant Physiol. Biochem.* 209, 108565. doi: 10.1016/j.plaphy.2024.108565
- Zou, Q. (2000). *Plant Physiology Experiments Guide* (Beijing, China: China Agriculture Press).